Quantifying landslide frequency and sediment residence time in the Nepal Himalaya

Whipp, David Michael

2019-04

Whipp , D M & Ehlers , T 2019 , ' Quantifying landslide frequency and sediment residence time in the Nepal Himalaya ' , Science Advances , vol. 5 , no. 4 , 3482 . https://doi.org/10.1126/sciadv.aav3482

http://hdl.handle.net/10138/302834
https://doi.org/10.1126/sciadv.aav3482

GEOLOGY

Quantifying landslide frequency and sediment residence time in the Nepal Himalaya

D. M. Whipp[1]* and T. A. Ehlers[2]

Quantifying how Earth surface processes interact with climate, tectonics, and biota has proven challenging, in part due to the stochastic nature of erosion and sedimentation. Landsliding is a common stochastic erosional process that may account for >50% of the sediment produced in steep mountainous landscapes. Here, we calculate the effects of landsliding and the residence time of sediment in a steep drainage basin in the Nepal Himalaya using a numerical model of landslide erosion combined with published cooling age distributions from two river sediment samples collected several years apart. We find that the difference in the two samples can be explained by landsliding and that the age distributions suggest that the residence time of sediment in the catchment is no greater than 50 years. This sensitivity to landsliding thus offers potential to improve our understanding of stochastic erosional processes, and further suggests that sediment is rapidly evacuated from steep mountainous drainage basins.

INTRODUCTION

Understanding how different erosional processes (e.g., fluvial, glacial, and hillslope) modify topography is a necessary step toward elucidating the interactions of weather and climate, tectonic activity, and biological processes (*1*). However, determining how specific processes contribute to the evolution of topography is complicated because some erosional or depositional processes are continuous, while others are stochastic (*2*). Landslide erosion and sedimentation are examples of stochastic surface processes and are important because they pose some of the greatest hazards to people living in mountainous regions. Detrital thermochronology offers a potential solution to understanding the stochastic sediment supply by landslides and has been successfully applied to understand how a distribution of mineral cooling ages reflects variations in fluvial (*3*, *4*), glacial (*5*, *6*), and combined hillslope-fluvial erosional processes (*7*). Here, we demonstrate how shallow landsliding produces clear peaks in the distributions of detrital thermochronometer ages measured in river sediments downstream. Furthermore, we show how the variability in catchment cooling ages can be used to estimate the residence time of landslide-derived sediment in mountainous catchments. To do this, we consider the influences of landslide-derived sediment storage and mixing with sediment produced by other processes.

Thermochronometer data record the time since a rock sample passed through its effective closure temperature in Earth's crust, which varies for different thermochronometer systems. For the muscovite $^{40}Ar/^{39}Ar$ (MAr) thermochronometer, the effective closure temperature ranges from 300°C up to as high as 550°C for different cooling rates (*8*–*10*). A fundamental aspect of bedrock thermochronology is that ages commonly increase with sample elevation in a catchment because the distance (and time) traveled from a closure temperature to the surface typically increases with elevation (*11*). This age-elevation relationship forms the basis of detrital thermochronometer interpretation, which frequently uses the distribution of ages measured in a sediment sample to determine the elevation from which the sediment was sourced (*12*).

Landsliding is the dominant erosional process providing sediment to rivers in steep mountainous catchments, yet sediment mobilized by landslides comes from point sources within a drainage basin and thus may not be representative of the distribution of bedrock ages in the upstream drainage area. It has been estimated that >50% of the sediment produced in steep catchments like those of the Himalaya or Southern Alps (New Zealand) is the result of shallow bedrock landslides (*13*, *14*). The sediment from localized landslide sources can provide a large number of minerals with similar thermochronometer ages in a detrital age distribution (Fig. 1, A and B). If this sediment does not reside and mix in the catchment for enough time (≥100 years), it is possible that minerals in the river sediment reflect individual upstream point sources. Thus, the age range for detritus produced by landsliding could be similar to other erosional mechanisms (Fig. 1B), but comparison of the observed age distributions to predictions from models that assume uniform catchment erosion may be misleading.

We estimate the production of landslide-derived sediment and its residence time in a steep catchment using a simple numerical model of landslide erosion combined with previously published bedrock age predictions from a three-dimensional (3D) thermokinematic numerical model (Fig. 2) (*15*). The distribution of grain ages in a detrital thermochronometer sample is sensitive not only to surface processes such as landsliding that determine the elevation from which river sediment is derived but also to the long-term denudation and tectonic history of a catchment (Fig. 2, A and B). To simulate these combined effects, we use the 3D thermokinematic numerical model Pecube (*16*) modified to calculate detrital thermochronometer age distributions for a modern river sediment sample with a stochastic distribution of landslides in the catchment (Fig. 2C) (*15*). The landslide model is used to assess how bedrock landsliding affects detrital thermochronometer age distributions for landslide-generated sediment that accumulates over varying sediment residence times in the catchment, in different drainage basin sizes, and that is mixed with sediment produced by other erosional mechanisms. The residence time in our models is defined as the time sediment grains remain within the catchment as part of the population of minerals that could be dated in a random sample. Note that our definition assumes effectively no long-term sediment storage in the catchment, which we further justify in Discussion. We focus on the Nyadi River drainage basin (Fig. 1C), a tributary to the Marsyandi River in central Nepal, where detrital MAr thermochronometer age predictions with uniform basin erosion reproduce the age distribution from a sample collected in 2002 (*17*), but do not reproduce an earlier sample from 1997 (Fig. 1D) (*18*).

[1]Institute of Seismology, Department of Geosciences and Geography, University of Helsinki, Helsinki, Finland. [2]Department of Geosciences, University of Tübingen, Tübingen, Germany. *Corresponding author. Email: david.whipp@helsinki.fi

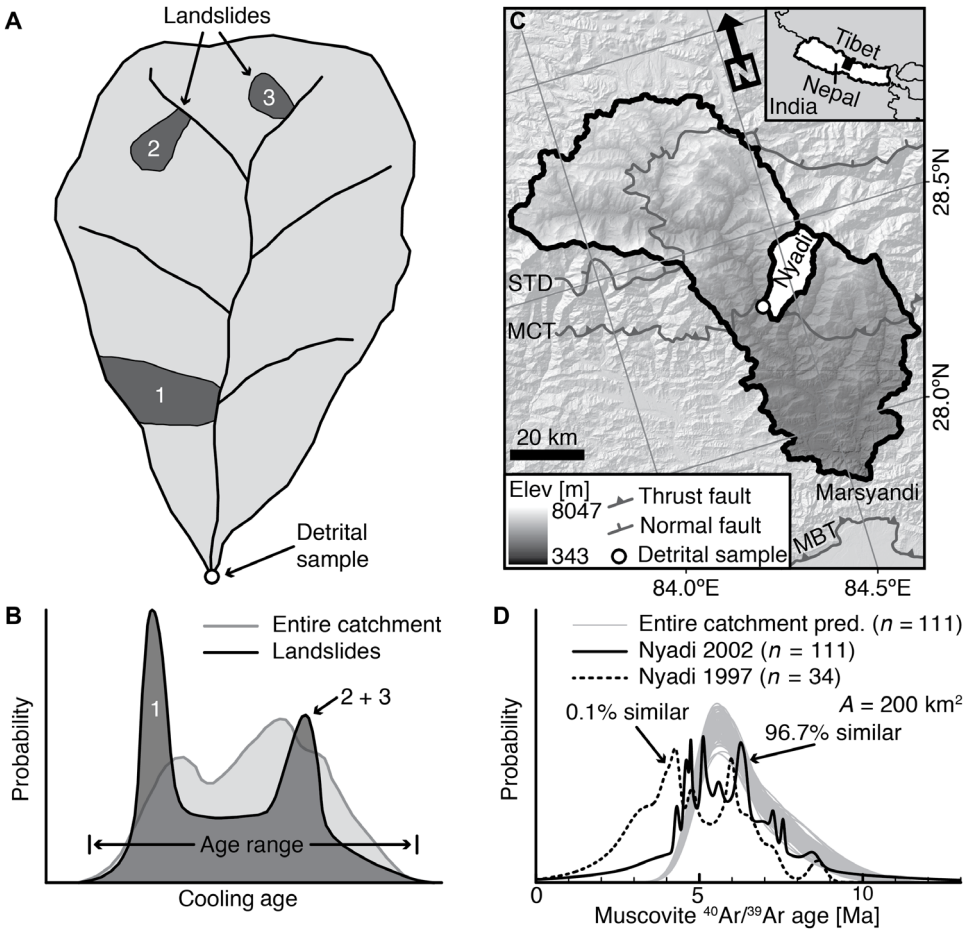

Fig. 1. Influence of bedrock landslides on a detrital age distribution, and predicted and observed age distributions from the Nyadi catchment in central Nepal. (**A**) A river sediment sample in a drainage basin may record denudation of the entire basin (light gray) or sediment generated dominantly by bedrock landslides (dark gray), producing (**B**) significantly different age distributions with the same age range [after Stock *et al*. (*3*)]. (**C**) Shaded relief digital elevation model of the Marsyandi drainage basin (heavy black border) in central Nepal with major tectonic structures and the location of the ~200-km^2 Nyadi catchment (white fill). MBT, Main Boundary Thrust; MCT, Main Central Thrust; STD, South Tibetan Detachment. (**D**) Predicted detrital MAr age distributions (gray) based on uniform basin denudation show variable goodness of fit to the observed age distributions (black solid, dashed lines), with very similar ages to the 2002 sample and age distributions that do not match the 1997 sample. The 2002 data are from Ruhl and Hodges (*17*), and the 1997 data are from Brewer *et al*. (*18*).

The influence of bedrock landsliding on detrital thermochronometer ages is determined by comparing predicted age distributions for different sediment residence times in the catchment. We consider residence times between t_r = 1 and 1000 years and do not vary any other model parameters. For each residence time, 10,000 age distributions are calculated using n = 111 predicted ages and compared to the observed ages (also n = 111) from the Nyadi catchment (Fig. 1, C and D) (*17*). Details of the numerical modeling approach are provided in Materials and Methods and the Supplementary Materials.

RESULTS

Effects of landsliding on detrital age distributions

For short sediment residence times (1 and 10 years), small regions of the drainage basin are sampled by landslides and the predicted age distributions exhibit a poor fit to the observed age distribution for the Nyadi catchment. With a residence time of t_r = 1 year, the predicted synoptic probability density functions (SPDFs) (*17*) are highly variable and poorly fit the observed age distribution; only 0.2% of the predicted SPDFs are equal to the observed age distribution (Fig. 3A, gray lines). The peak ages of the predicted SPDFs range from ~5 to 10 million years (Ma), distributed nearly equally across that range. The variability is the result of few landslides that sample ages from only a small portion of the drainage area, providing small clusters of similar ages from each landslide. The age variability decreases as the residence time is increased to t_r = 10 years, with predicted peak ages of ~5 to 8 Ma that cluster close to the prominent peak at 5 Ma (Fig. 3B). This reduction in variation is due to sampling a larger fraction of the catchment over the 10-year residence time. Although the longer residence time results in an improved fit to the observed age data (8.2% of the predicted age SPDFs are equal to the observed), the fit is still quite poor for short residence times (≤10 years).

As more of the drainage area is sampled by landslides occurring over longer residence times (100 and 1000 years), the fit to the observed age distribution improves and becomes more similar to that observed for uniform denudation of the catchment (Figs. 1D and 3, C and D). With a residence time of t_r = 100 years, nearly all of the peak ages for the predicted SPDFs are between 5 and 6 Ma, providing a better representation of the observed age data, as indicated by the larger percentage of predicted and observed SPDFs that are statistically indistinguishable (39.5%; Fig. 3C). For t_r = 1000 years, the variability in the predicted

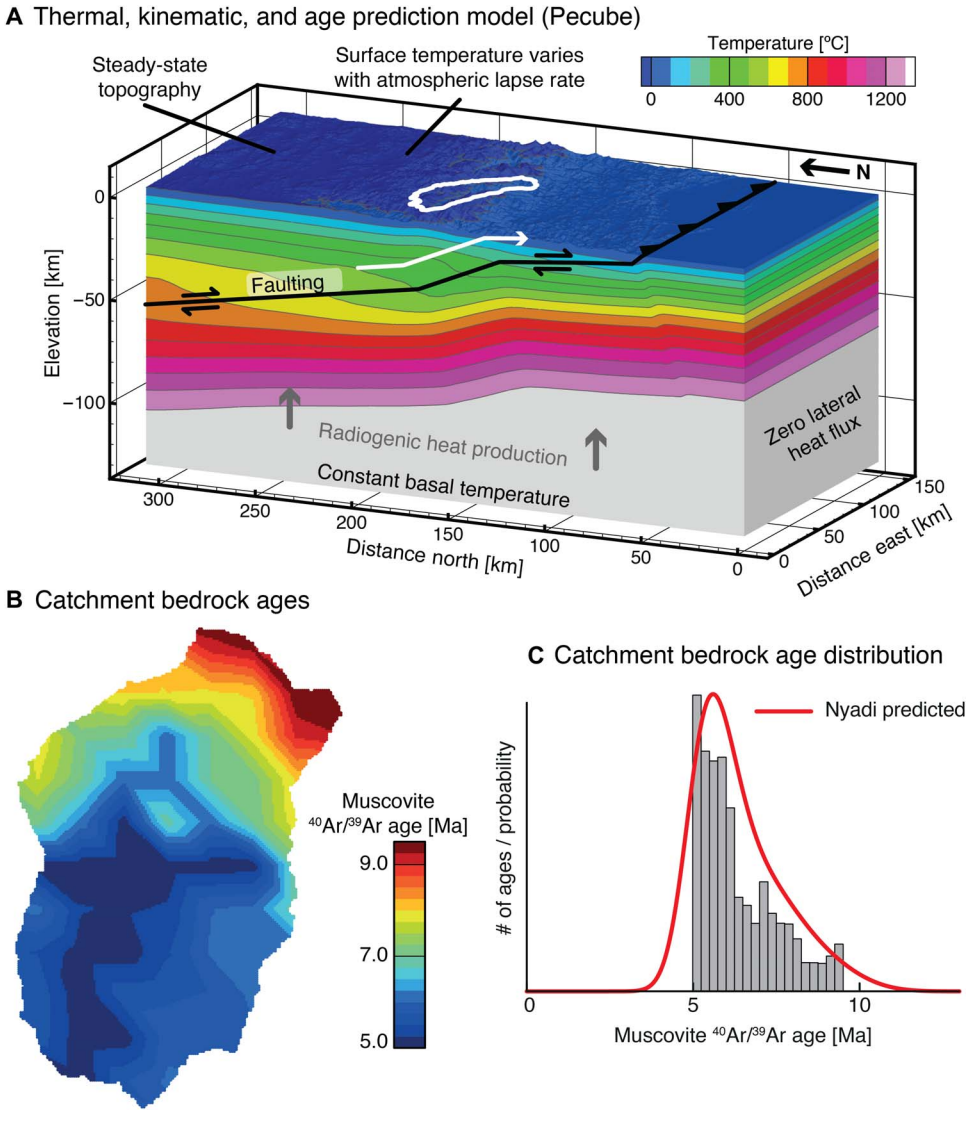

Fig. 2. Overview of catchment bedrock age prediction. (**A**) Example 3D thermokinematic numerical model of the Marsyandi River region including the effects of active thrusting on the model equivalent of the Main Himalayan Thrust [see Whipp *et al.* (*15*) for model design details]. Thermochronometer ages are predicted across the entire model surface as particles travel toward the surface along their exhumation pathways (e.g., white arrow). (**B**) Example of a catchment subsample of predicted MAr bedrock ages. (**C**) Predicted SPDF ($SPDF_p$) for all catchment bedrock ages. Age prevalence in the $SPDF_p$ is scaled by the instantaneous exhumation rate at the surface in the thermokinematic numerical model (A).

SPDFs is quite limited, all sharing a similar peak age and form. In this case, 57.3% of the predicted and observed age distributions are equal, and the predicted SPDFs are very similar to those calculated for uniform denudation of the entire catchment (Figs. 1D and 3D). This shows that landslide-driven erosion approaches uniform catchment erosion for long residence times ($t_r \geq 1000$ years).

Sensitivity to basin size and other erosional processes

Smaller drainage basins (≤25 km^2) appear to be less sensitive to the effects of shallow landsliding, at least in rapidly eroding landscapes. For three subbasins in the Nyadi catchment with areas of ~100, ~25, and ~5 km^2 (Fig. 4A), we calculated age distributions and compared them to the predicted age distribution for uniform erosion of the subbasin for different sediment residence times. At residence times of $t_r \leq$ 25 years, predicted age distributions for the entire Nyadi catchment and its upper half (A = 103.2 km^2) are equal to those resulting from uniform basin erosion less than ~50% of the time, again suggesting a strong effect of landsliding for short residence times. Unexpectedly, the smaller subbasins (A = 5 and 25 km^2) are different, with at least ~75% of the landslide-produced age distributions being equal to that for uniform subbasin erosion for all residence times (Fig. 4A). This observation is unexpected because small basins should be particularly sensitive to individual landslides based on the landslide frequency-area relationship (Eq. 1 and fig. S1C), which predicts that no landslides should occur in under 50 to 100 years for basins with drainage areas of 5 km^2 or 5 to 10 years for a 25-km^2 basin area. The apparent lack of signal for these small, rapidly eroding basins reflects their relatively small range of bedrock thermochronometer ages.

In contrast to landsliding, many other hillslope erosional processes are not stochastic and thus contribute a more representative sample of

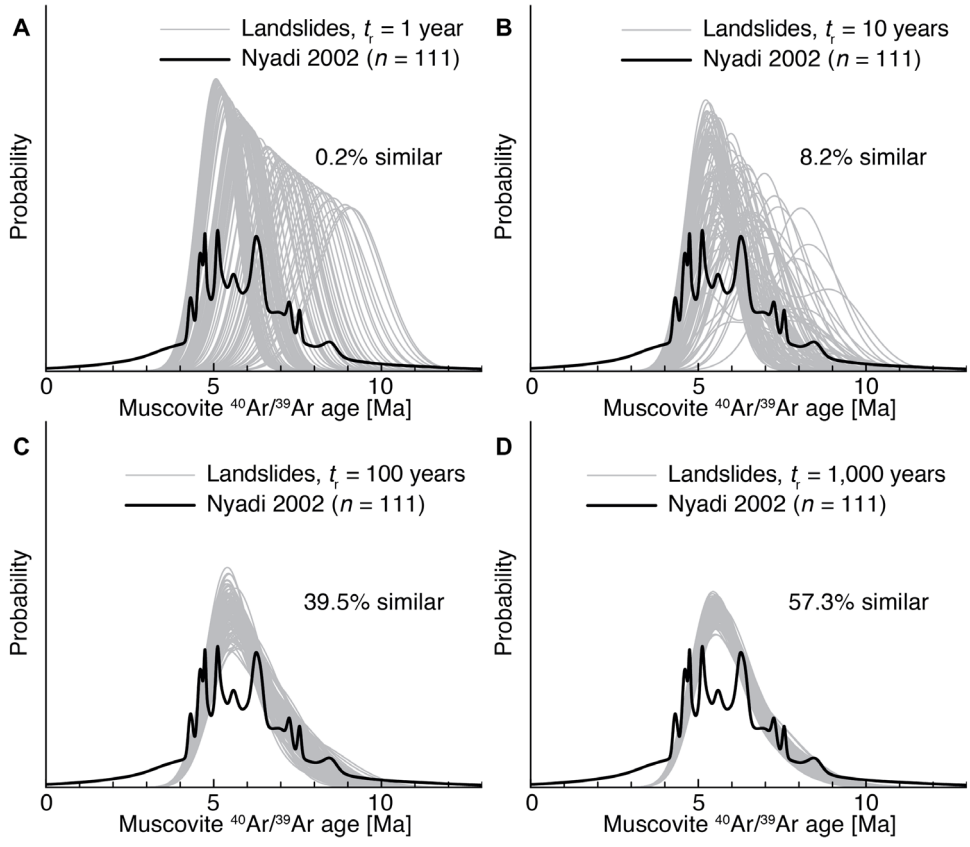

Fig. 3. Predicted MAr age distributions for varying sediment residence time t_r and observed ages from the Nyadi catchment. One hundred of 10,000 predicted age distributions (gray) for (**A**) t_r = 1 year, (**B**) t_r = 10 years, (**C**) t_r = 100 years, and (**D**) t_r = 1000 years. The percent similarity refers to the percentage of predicted age distributions that pass the two-sample Kuiper's test [see Press *et al*. (*33*) and the Supplementary Materials]. Decreasing variation in peak age is the result of an increase in the fraction of the drainage basin that is sampled by landslide-generated sediment as t_r increases. Data are from Ruhl and Hodges (*17*). The predicted age SPDFs are smoother than the observed age distribution because they were created using the median percent uncertainty in the observed ages (σ = 10.9%), whereas the percent uncertainty for individual observed ages ranges from <1% to >1000%. Abbreviations as in Fig. 2 caption.

the sediment produced across the drainage basin. We simulated mixing of the contributions of landslide-mobilized sediment and that contributed by erosional processes that occur across the entire basin by combining the predictions from the landsliding model with those for uniform basin erosion using a landsliding sediment mixing factor f (Fig. 4B), where $f = 0$ corresponds to uniform basin erosion and landslides produce all of the basin sediment when $f = 1$. As above, the impact of bedrock landslides on catchment sediment is strongly controlled by the residence time of sediment in the catchment (Fig. 3). The influence of landslides can be detected when landslides produce 15 to 25% of the catchment sediment for residence times of 1 to 10 years (Fig. 4B). For longer residence times of 100 to 1000 years, the impact of bedrock landsliding may only be detected when landslides produce 60 to 80% of the catchment sediment, for catchments of similar size to the Nyadi (Fig. 4B).

DISCUSSION

The degree to which landslide-produced sediments are representative of the upstream distribution of bedrock thermochronometer ages strongly depends on the residence time, which is difficult to determine for steep catchments where shallow landsliding is common. We observed a strong impact of individual landslides on detrital thermochronometer age distributions for basins on the order of 100 km^2 for short residence times (≤10 years) and reduced sensitivity for longer residence times (>100 years), where a larger total number of landslides would be expected to sample more of the bedrock exposed in the catchment.

There are several observations that support short sediment residence times in steep landscapes, particularly in the central Himalaya. First, studies of sediment fluxes resulting from landslides triggered by large earthquakes suggest a considerable transient increase in sediment discharge following those events (*19*–*21*). For example, the sediment discharge following the M_W (moment magnitude) 7.6 ChiChi earthquake was enhanced for ~6 years before returning to pre-earthquake levels, suggesting that much of the mobilized sediment that reached the rivers was transported out of the catchments in that time (*19*). Furthermore, fine sediment fluxes were also elevated following the 2008 Wenchuan earthquake, with estimated sediment residence times typically less than ~10 years for drainage areas up to ~1000 km^2 (*20*). Second, elsewhere in the Himalaya, sediment with grain sizes below 1 mm comprises only a small fraction (<15%) of material found in channel bars (*22*, *23*), suggesting minimal storage of this size fraction within these catchments. This observation suggests that much of the finer sediment, which is often targeted for detrital geochronology, is transported downstream annually during the summer monsoon season. Similar observations have

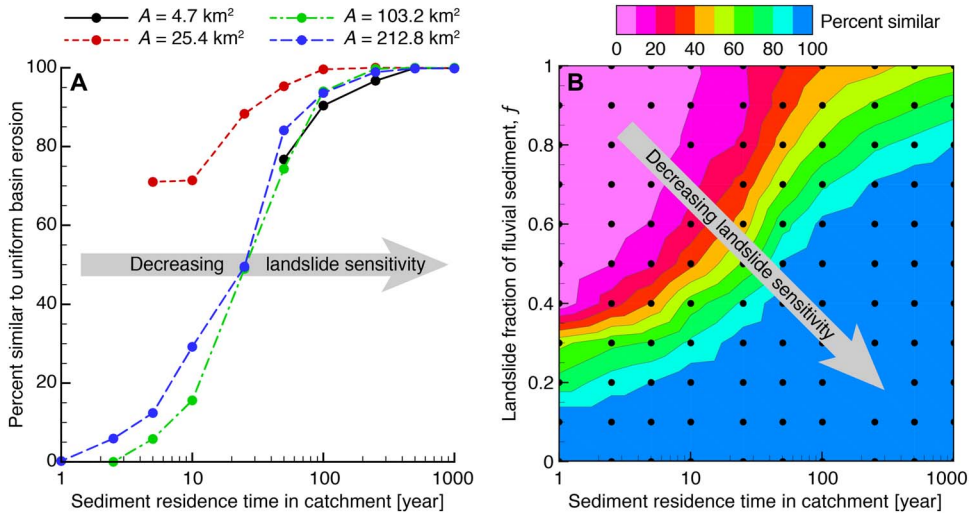

Fig. 4. The effects of bedrock landsliding on predicted detrital age distributions as a function of drainage basin area, sediment residence time, and fluvial sediment mixing. (**A**) Predicted landslide-generated age distributions from the whole Nyadi catchment (blue) and three subcatchments (green, red, and black) show increasing agreement with equivalent predicted age distributions for uniform basin denudation as the sediment residence time t_r increases. (**B**) Mixing of landslide sediment with sediment generated by other hillslope processes shows that a lower fraction of landslide-derived sediment increases the probability that the predicted age distributions and the 2002 observed age distribution (*17*) are statistically equal, as does increasing the sediment residence time. Black filled circles indicate results from individual models.

been made in the Narayani River basin to which the Nyadi is a tributary, where transport of suspended sediment derived from hillslopes during the monsoon season is very rapid with minimal storage (*24*). Although the residence time of coarser sediment transported as bed load appears to be tens to hundreds of years (*25*), the residence time of suspended sediment in mountainous catchments appears quite short. Last, the short residence time is supported by limited storage of sediment in steep catchments in the central Himalaya compared to those in the eastern and western Himalaya (*26*). There are valley-filling sediments present in the central Himalaya, but mainly at lower elevations downstream of the steepest parts of the landscape.

If the residence time of landslide-produced sediment in steep mountainous catchments is short (~10 years or less), a reasonable explanation for the difference in the 1997 and 2002 detrital age distributions from the Nyadi catchment (Fig. 1D) (*17*, *18*) is that the analyzed sediment was sourced from bedrock landslides in different parts of the basin. We predict ~3 Ma of variability in the MAr peak ages in the Nyadi catchment (Fig. 3B), with a residence time of 10 years, which is larger than the observed offset in the peak ages in the 1997 and 2002 Nyadi catchment samples (<1 Ma) and the difference in the age of the youngest peaks (~1.5 Ma; Fig. 1D).

Although few studies exist with detrital thermochronology samples collected in multiple years from the same basin, there is evidence that sediment analyzed in some previous studies may have been sourced from point sources such as bedrock landslides or rockfalls. Detrital age distributions from samples collected in 1997 and 2002 in the Marsyandi River (*17*, *18*), the trunk stream into which the Nyadi drains, do not reproduce and are statistically different. Although it is difficult to attribute the cause of this difference to landsliding from the age distributions alone, the fact that the two samples have similar age ranges but different probability distributions is consistent with sediment sourced from landslides. Furthermore, an abundance of young ages observed in one detrital sample from the White Mountains of California (*27*) was inconsistent with the observed bedrock age range in the catchment. This inconsistency was attributed to a local rockfall at low elevation in the study catchment.

Similar sensitivity to stochastic erosional processes has been observed in studies using cosmogenic radionuclide dating, where the issue of sample replicability has received greater attention. Cosmogenic radionuclides in bedrock form by interaction between cosmic rays and various minerals within ~2 m of the Earth's surface [e.g., (*28*)], making them highly sensitive to processes affecting Earth's shallow surface such as landsliding. In a recent meta-analysis, Sosa Gonzalez *et al.* (*29*) reviewed a number of past cosmogenic radionuclide studies, finding that samples are less likely to replicate as landscape steepness increases. Sample replication was found to be worst when basins are small (<210 km^2) and landsliding or other mass movements occur frequently. This is consistent with past studies modeling the effects of landsliding on cosmogenic radionuclides (*30*, *31*), where the greatest sensitivity to landsliding was observed in small catchments. A similar sensitivity to stochastic erosion was observed in the western Himalaya (*22*), where variability in cosmogenic radionuclide concentrations was attributed to stochastic sediment input upstream. This case is notable because sensitivity to stochastic erosion events is found even in basins with areas in excess of 10,000 km^2.

Combined, these observations suggest that different erosional mechanisms and sediment residence times produce a signal in detrital thermochronometer data. In steep mountainous catchments where bedrock landsliding is active, the stochastic nature of landslides may bias the calculated age distributions from modern river sediment (Fig. 5). In the examples provided here, this effect appears only when the residence time of sediment in the catchment is short (<50 years), but it is possible that catchments experiencing slower average denudation rates may have a larger age range and greater sensitivity to landsliding (Fig. 5A). In contrast, catchments with long sediment residence times, low relief, or a small range in bedrock ages are not likely to be sensitive to stochastic erosion (Fig. 5B). Thus, the results presented here demonstrate a new potential for thermochronometer dating

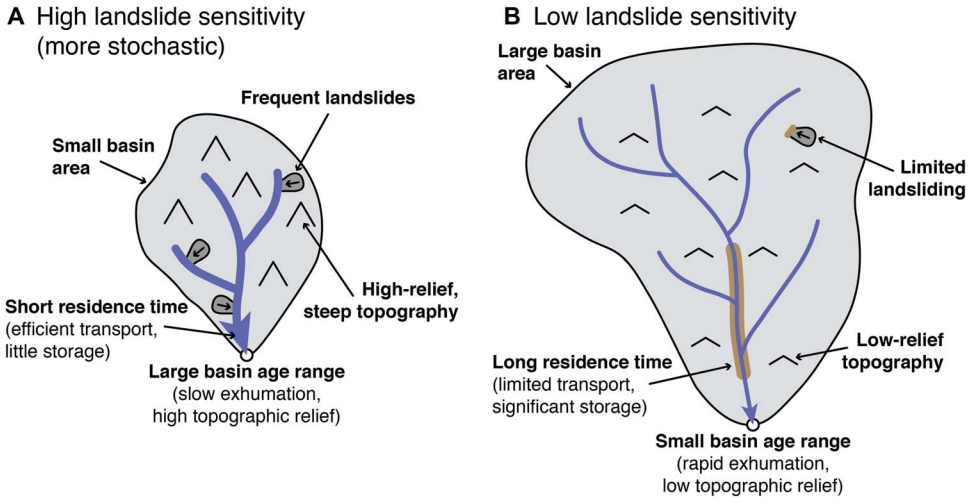

Fig. 5. Factors affecting the sensitivity of detrital thermochronometers to stochastic erosion processes. (**A**) Factors that increase sensitivity of detrital thermochronometers to stochastic erosion include a small basin area, frequent erosion by landsliding or other stochastic mass wasting processes, high-relief and/or steep topography, rapid evacuation of catchment sediment from the basin (heavy blue lines), and a large range of ages in the catchment bedrock. (**B**) In contrast, detrital thermochronometers are less likely to be affected by stochastic erosion when the basin area is large, erosion by landslides is infrequent or landslide deposits remain perched on hillslopes, the topographic relief is low, fluvial evacuation is inefficient (thinner blue lines) and large volumes of sediment are stored in the catchment for decades or more (brown regions), or the range of ages in the catchment bedrock is small.

techniques to quantify landslide activity and sediment transport on the Earth's surface.

MATERIALS AND METHODS

The crustal scale thermal and kinematic model used the present-day topography of the study area and the deformation history determined from previous work (*15*, *32*) to predict spatial variations in cooling ages. Monte Carlo sampling was used to extract a subset of n ages from the population of catchment ages and create a predicted SPDF (*17*) that accounts for spatially variable exhumation rates across the catchment by dividing the calculated SPDF by the average catchment exhumation rate (*15*). For each Monte Carlo iteration and predicted SPDF, a predicted cumulative SPDF was calculated and compared to the observed age distribution using the two-sample Kuiper's test (*33*), with a significance level of $\alpha = 0.05$. The results were recorded to log the percentage of predicted cumulative SPDFs that are statistically indistinguishable from the observed age distribution. Additional details of the model are provided in the Supplementary Materials.

The influence of bedrock landsliding on the detrital age distributions was simulated using a simple landsliding model with random landslide locations within a given catchment and a power-law frequency-area relationship. Landslide size follows the empirical power-law frequency-area relationship of Hovius *et al.* (*13*)

$$n_c(A \geq A_c) = \kappa(A_c/A_r)^{-\beta}A_r \quad (1)$$

which states that the number of landslides n_c with an area larger than A_c in a reference area A_r is a function of the landsliding rate per unit area per year κ and the power-law exponent β. We calculated landslide occurrence for landslide areas A_c of 0.005 to 38.5 km^2 using a reference area of $A_r = 1$ km^2 and with a preferred power-law exponent $\beta = 1.16$ from Hovius *et al.* (*13*). The landsliding rate κ was scaled to produce an average surface denudation rate equal to the rock uplift rate in Pecube (2.5 mm/a) following the method described by Niemi *et al.* (*30*). Landslide-produced thermochronometer ages accumulate as sediment is stored in the catchment for a residence time t_r. Bedrock thermochronometer ages do not vary with depth for the landslide-sampled sediment.

SUPPLEMENTARY MATERIALS

Supplementary material for this article is available at http://advances.sciencemag.org/cgi/content/full/5/4/eaav3482/DC1

Fig. S1. Overview of landslide age prediction.

Fig. S2. Satellite imagery of landslides in the Nyadi catchment.

Reference (*34*)

REFERENCES AND NOTES

1. W. E. Dietrich, J. T. Perron, The search for a topographic signature of life. *Nature* **439**, 411–418 (2006).
2. J. W. Kirchner, R. C. Finkel, C. S. Riebe, D. E. Granger, J. L. Clayton, J. G. King, W. F. Megahan, Mountain erosion over 10 yr, 10 k.y., and 10 m.y. time scales. *Geology* **29**, 591–594 (2001).
3. G. M. Stock, T. A. Ehlers, K. A. Farley, Where does sediment come from? Quantifying catchment erosion with detrital apatite (U-Th)/He thermochronometry. *Geology* **34**, 725–728 (2006).
4. D. McPhillips, M. T. Brandon, Using tracer thermochronology to measure modern relief change in the Sierra Nevada, California. *Earth Planet. Sci. Lett.* **296**, 373–383 (2010).
5. L. M. Tranel, J. A. Spotila, M. J. Kowalewski, C. M. Waller, Spatial variation of erosion in a small, glaciated basin in the Teton Range, Wyoming, based on detrital apatite (U-Th)/He thermochronology. *Basin Res.* **23**, 571–590 (2011).
6. T. A. Ehlers, A. Szameitat, E. Enkelmann, B. J. Yanites, G. J. Woodsworth, Identifying spatial variations in glacial catchment erosion with detrital thermochronology. *J. Geophys. Res. Earth Surf.* **120**, 1023–1039 (2015).
7. C. E. Lukens, C. S. Riebe, L. S. Sklar, D. L. Shuster, Grain size bias in cosmogenic nuclide studies of stream sediment in steep terrain. *J. Geophys. Res. Earth Surf.* **121**, 978–999 (2016).
8. T. M. Harrison, J. Célérier, A. B. Aikman, J. Hermann, M. T. Heizler, Diffusion of ^{40}Ar in muscovite. *Geochim. Cosmochim. Acta* **73**, 1039–1051 (2009).
9. T. A. Ehlers, T. Chaudhri, S. Kumar, C. W. Fuller, S. D. Willett, R. A. Ketcham, M. T. Brandon, D. X. Belton, B. P. Kohn, A. J. W. Gleadow, T. J. Dunai, F. Q. Fu, Computational tools for

low-temperature thermochronometer interpretation. *Rev. Mineral. Geochem.* **58**, 589–622 (2005).
10. K. V. Hodges, in *Treatise on Geochemistry*, K. K. Turekian, Ed. (Elsevier, ed. 2, 2014), pp. 281–308.
11. P. G. Fitzgerald, E. Stump, T. F. Redfield, Late Cenozoic uplift of Denali and its relation to relative plate motion and fault morphology. *Science* **259**, 497–499 (1993).
12. J. D. Stock, D. R. Montgomery, Estimating palaeorelief from detrital mineral age ranges. *Basin Res.* **8**, 317–327 (1996).
13. N. Hovius, C. P. Stark, P. A. Allen, Sediment flux from a mountain belt derived by landslide mapping. *Geology* **25**, 231–234 (1997).
14. P. L. Barnard, L. A. Owen, M. C. Sharma, R. C. Finkel, Natural and human-induced landsliding in the Garhwal Himalaya of northern India. *Geomorphology* **40**, 21–35 (2001).
15. D. M. Whipp Jr., T. A. Ehlers, J. Braun, C. D. Spath, Effects of exhumation kinematics and topographic evolution on detrital thermochronometer data. *J. Geophys. Res. Earth Surf.* **114**, F04021 (2009).
16. J. Braun, P. van der Beek, P. Valla, X. Robert, F. Herman, C. Glotzbach, V. Pedersen, C. Perry, T. Simon-Labric, C. Prigent, Quantifying rates of landscape evolution and tectonic processes by thermochronology and numerical modeling of crustal heat transport using PECUBE. *Tectonophysics* **524–525**, 1–28 (2012).
17. K. W. Ruhl, K. V. Hodges, The use of detrital mineral cooling ages to evaluate steady state assumptions in active orogens: An example from the central Nepalese Himalaya. *Tectonics* **24**, TC4015 (2005).
18. I. D. Brewer, D. W. Burbank, K. Hodges, Downstream development of a detrital cooling-age signal: Insights from $^{40}Ar/^{39}Ar$ muscovite thermochronology in the Nepalese Himalaya. *Geol. Soc. Am. Spec. Paper* **398**, 321–338 (2006).
19. N. Hovius, P. Meunier, C.-W. Lin, H. Chen, Y.-G. Chen, D. Simon, M.-J. Horng, M. Lines, Prolonged seismically induced erosion and the mass balance of a large earthquake. *Earth Planet. Sci. Lett.* **304**, 347–355 (2011).
20. J. Wang, Z. Jin, R. G. Hilton, F. Zhang, A. L. Densmore, G. Li, A. J. West, Controls on fluvial evacuation of sediment from earthquake-triggered landslides. *Geology* **43**, 115–118 (2015).
21. J. S. Kargel, G. J. Leonard, D. H. Shugar, U. K. Haritashya, A. Bevington, E. J. Fielding, K. Fujita, M. Geertsema, E. S. Miles, J. Steiner, E. Anderson, S. Bajracharya, G. W. Bawden, D. F. Breashears, A. Byers, B. Collins, M. R. Dhital, A. Donnellan, T. L. Evans, M. L. Geai, M. T. Glasscoe, D. Green, D. R. Gurung, R. Heijenk, A. Hilborn, K. Hudnut, C. Huyck, W. W. Immerzeel, J. Liming, R. Jibson, A. Kääb, N. R. Khanal, D. Kirschbaum, P. D. A. Kraaijenbrink, D. Lamsal, L. Shiyin, L. Mingyang, D. McKinney, N. K. Nahirnick, N. Zhuotong, S. Ojha, J. Olsenholler, T. H. Painter, M. Pleasants, K. C. Pratima, Q. I. Yuan, B. H. Raup, D. Regmi, D. R. Rounce, A. Sakai, S. Donghui, J. M. Shea, A. B. Shrestha, A. Shukla, D. Stumm, M. van der Kooij, K. Voss, W. Xin, B. Weihs, D. Wolfe, W. Lizong, Y. Xiaojun, M. R. Yoder, N. Young, Geomorphic and geologic controls of geohazards induced by Nepal's 2015 Gorkha earthquake. *Science* **351**, aac8353 (2016).
22. E. H. Dingle, H. D. Sinclair, M. Attal, Á. Rodés, V. Singh, Temporal variability in detrital ^{10}Be concentrations in a large Himalayan catchment. *Earth Surf. Dynam.* **6**, 611–635 (2018).
23. E. H. Dingle, H. D. Sinclair, M. Attal, D. T. Milodowski, V. Singh, Subsidence control on river morphology and grain size in the Ganga Plain. *Am. J. Sci.* **316**, 778–812 (2016).
24. G. P. Morin, J. Lavé, C. France-Lanord, T. Rigaudier, A. P. Gajurel, R. Sinha, Annual sediment transport dynamics in the Narayani basin, Central Nepal: Assessing the impacts of erosion processes in the annual sediment budget. *J. Geophys. Res. Earth Surf.* **123**, 2341–2376 (2018).
25. B. J. Yanites, G. E. Tucker, K. J. Mueller, Y.-G. Chen, How rivers react to large earthquakes: Evidence from central Taiwan. *Geology* **38**, 639–642 (2010).
26. J. H. Blöthe, O. Korup, Millennial lag times in the Himalayan sediment routing system. *Earth Planet. Sci. Lett.* **382**, 38–46 (2013).
27. P. Vermeesch, Quantitative geomorphology of the White Mountains (California) using detrital apatite fission track thermochronology. *J. Geophys. Res. F Earth Surf.* **112**, F03004 (2007).
28. J. C. Gosse, F. M. Phillips, Terrestrial in situ cosmogenic nuclides: Theory and application. *Quat. Sci. Rev.* **20**, 1475–1560 (2001).
29. V. Sosa Gonzalez, A. H. Schmidt, P. R. Bierman, D. H. Rood, Spatial and temporal replicability of meteoric and in situ ^{10}Be concentrations in fluvial sediment. *Earth Surf. Process. Landf.* **42**, 2570–2584 (2017).
30. N. A. Niemi, M. Oskin, D. W. Burbank, A. M. Heimsath, E. J. Gabet, Effects of bedrock landslides on cosmogenically determined erosion rates. *Earth Planet. Sci. Lett.* **237**, 480–498 (2005).
31. B. J. Yanites, G. E. Tucker, R. S. Anderson, Numerical and analytical models of cosmogenic radionuclide dynamics in landslide-dominated drainage basins. *J. Geophys. Res. F Earth Surf.* **114**, F01007 (2009).
32. D. M. Whipp Jr., T. A. Ehlers, A. E. Blythe, K. W. Huntington, K. V. Hodges, D. W. Burbank, Plio-Quaternary exhumation history of the central Nepalese Himalaya: 2. Thermokinematic and thermochronometer age prediction model. *Tectonics* **26**, TC3003 (2007).
33. W. H. Press, S. A. Teukolsky, W. T. Vetterling, B. P. Flannery, M. Metcalf, *Numerical Recipes in Fortran 90: The Art of Parallel Scientific Computing* (Cambridge Univ. Press, 1996), vol. 2.
34. P. Bettinelli, J.-P. Avouac, M. Flouzat, F. Jouanne, L. Bollinger, P. Willis, G. R. Chitrakar, Plate motion of India and interseismic strain in the Nepal Himalaya from GPS and DORIS measurements. *J. Geodesy* **80**, 567–589 (2006).

Acknowledgments: We are grateful to I. Brewer, D. Burbank, K. Hodges, and K. Huntington for providing the data analyzed in this work. The manuscript benefitted from thoughtful comments from A. Schmidt and an anonymous reviewer. **Funding:** This work was partially supported by Academy of Finland Academy Project 276513 to D.M.W. and European Research Council (ERC) Consolidator Grant number 615703 to T.A.E. **Author contributions:** D.M.W. and T.A.E. designed the study and wrote the manuscript. D.M.W. wrote/modified the modeling software and conducted the numerical simulations. **Competing interests:** The authors declare that they have no competing interests. **Data and materials availability:** All data needed to evaluate the conclusions in the paper are present in the paper and/or the Supplementary Materials. Additional data are available from D.M.W. upon request.

Submitted 7 September 2018
Accepted 6 March 2019
Published 24 April 2019
10.1126/sciadv.aav3482

Citation: D. M. Whipp, T. A. Ehlers, Quantifying landslide frequency and sediment residence time in the Nepal Himalaya. *Sci. Adv.* **5**, eaav3482 (2019).

Science Advances

Quantifying landslide frequency and sediment residence time in the Nepal Himalaya

D. M. Whipp and T. A. Ehlers

Sci Adv **5** (4), eaav3482.
DOI: 10.1126/sciadv.aav3482